Vehicle System Dynamics Supplement 35 (2001), pp. 7-22

Influence of Locomotive Tractive Effort on the Forces Between Wheel and Rail

OLDRICH POLACH[1]

SUMMARY

For the complex simulation of dynamic behaviour of a locomotive in connection with drive dynamics and traction control, large longitudinal creep between wheel and rail and decreasing part of creep-force function behind adhesion limit have to be modelled. This needs an adaptation of models used for the computation of tangential forces between wheel and rail in vehicle dynamics. A fast method for the calculation of wheel-rail forces developed by the author was extended to get the properties mentioned above. The simulations with a locomotive model running in a curve with varying tractive force show the influence on the wheel-rail forces distribution and on the radial steering ability. Another application example presents the investigation of a complex mechatronic system of the traction control and vehicle dynamics. A comparison with the measurements confirms that the proposed method is suitable for the investigation of problems regarding the interaction of axle drive dynamics and vehicle behaviour.

1. INTRODUCTION

The standard methods of vehicle dynamics investigate only a part of the complex mechatronic systems of railway traction vehicles. To investigate e. g. influence of locomotive tractive effort on the forces between wheel and rail in the curve, influence of traction control parameters on the wheel-rail forces, on the dynamic behaviour of the locomotive or of the train set etc., the mechanics, electric and electronics have to be simulated simultaneously. The model of wheel-rail forces used in such computer simulations should contain the properties necessary for vehicle dynamics as well as for axle drive and traction control dynamics. This is not possible using the standard methods and needs an adaptation of models used for the computation of tangential forces between wheel and rail in vehicle dynamics. A fast method for the calculation of wheel-rail forces developed by the author was extended to get the properties mentioned above and verified by comparisons with measurements.

Application examples illustrate the influence of locomotive tractive effort on the forces between wheel and rail. Another application example presents the investigation of a complex mechatronic system of the traction control and vehicle dynamics using the co-simulation of ADAMS/Rail and MATLAB-SIMULINK.

[1] Adtranz Switzerland, Zürcherstr. 41, CH-8401 Winterthur, Switzerland

2. MODELS OF WHEEL-RAIL FORCES IN THE VEHICLE DYNAMICS SIMULATIONS

There are various methods for the computation of wheel-rail forces in railway vehicle dynamics. The best known methods can be divided into four groups:

- exact theory by Kalker (programme CONTACT)
- simplified theory by Kalker (programme FASTSIM)
- look-up tables
- simplified formulae and saturation functions.

The exact theory by Kalker (computer programme CONTACT [5]) has not been used in the simulations because of its very long calculation time.

The simplified theory used in Kalker's programme FASTSIM [3] is much faster than the exact theory, but the calculation time is still relatively long for on-line computation in complicated multi-body systems. FASTSIM is used e. g. in the railway vehicle simulation tools ADAMS/Rail, MEDYNA, SIMPACK, GENSYS, VOCO.

Another possibility for computer simulations consists in the use of look-up tables with saved pre-calculated values (ADAMS/Rail, VAMPIRE). Because of the limited data in the look-up table, there are differences to the exact theory as well. Large tables are more exact, but the searching in such large tables consumes calculation time.

Searching for faster methods some authors found approximations based on saturation functions (e.g. Vermeulen-Johnson [12], Shen-Hedrick-Elkins [11]). The calculation time using these approximations is short, but there are significant differences to the exact theory especially in the presence of spin. Simple approximations are often used as a fast and less exact alternative to standard methods (e. g. in MEDYNA, VAMPIRE, SIMPACK).

A very good compromise between the calculation time and the required accuracy allows a fast method for the computation of wheel-rail forces developed by the author [7], [8]. In spite of the simplifications used, spin is taken into consideration. Due to the short calculation time, the method can be used as a substitute for Kalker's programme FASTSIM to save computation time or instead of approximation functions to improve the accuracy.

The proposed method has been used in the simulations in different programmes since 1990. The algorithm is implemented in ADAMS/Rail as an alternative parallel to FASTSIM and to the Table-book. The calculation time is faster than FASTSIM's and usually faster than the Table-book as well. The proposed algorithm provides a smoothing of the contact forces in comparison with the Table-book and there are no convergence problems during the integration. The programme was tested as user routine in programmes: SIMPACK, MEDYNA, SIMFA and various user's own programmes with very good experience.

The proposed method assumes an ellipsoidal contact area with half-axes a, b and normal stress distribution according to Hertz. The maximum value of tangential stress τ at any arbitrary point is

$$\tau_{\max} = f \cdot \sigma \qquad (1)$$

where f - coefficient of friction,
σ - normal stress.

The coefficient of friction f is assumed constant in the whole contact area. The solution described in [7], [8] obtains the resultant tangential force (without spin) as

$$F = -\frac{2 \cdot Q \cdot f}{\pi} \left(\frac{\varepsilon}{1+\varepsilon^2} + \arctan \varepsilon \right) \qquad (2)$$

where Q - wheel load
f - friction coefficient
ε - gradient of the tangential stress in the area of adhesion

$$\varepsilon = \frac{2}{3} \frac{C \cdot \pi \cdot a^2 \cdot b}{Q \cdot f} s \qquad (3)$$

where C - proportionality coefficient characterising the contact elasticity
a, b - half-axes of the contact ellipse
s - creep

$$s = \sqrt{s_x^2 + s_y^2} \qquad (4a)$$

$$s_i = \frac{w_i}{V} \qquad i = x, y \qquad (4b)$$

where s_x, s_y - creep in longitudinal (x) and lateral (y) directions
w_x, w_y - creep (slip) velocity in longitudinal (x) and lateral (y) directions
V - vehicle speed.

Using the Kalker's linear theory to express the coefficient C, the equation (3) has then the form (in the case of only longitudinal creep)

$$\varepsilon = \frac{1}{4} \frac{G \cdot \pi \cdot a \cdot b \cdot c_{11}}{Q \cdot f} s_x \qquad (5)$$

where c_{11} - Kalker's coefficient for longitudinal direction [2].

The calculation of tangential forces for general case with combination of longitudinal and lateral creep and spin allows the computer code published in [8].

The proposed method was verified by making a comparison between curving behaviour calculations using for the computation of wheel-rail forces the programme FASTSIM and the proposed method, and by comparison with measurements. A model of the four axle SBB 460 locomotive of the Swiss Federal Railways was built by means of the simulation tool ADAMS/Rail. The locomotive design combines very

good curving performance with high maximal speed due to the coupling of wheelsets, realised by a mechanism with a torsional shaft assembled to the bogie frame. The model used in simulations consists of 51 rigid bodies and contains 266 degrees of freedom.

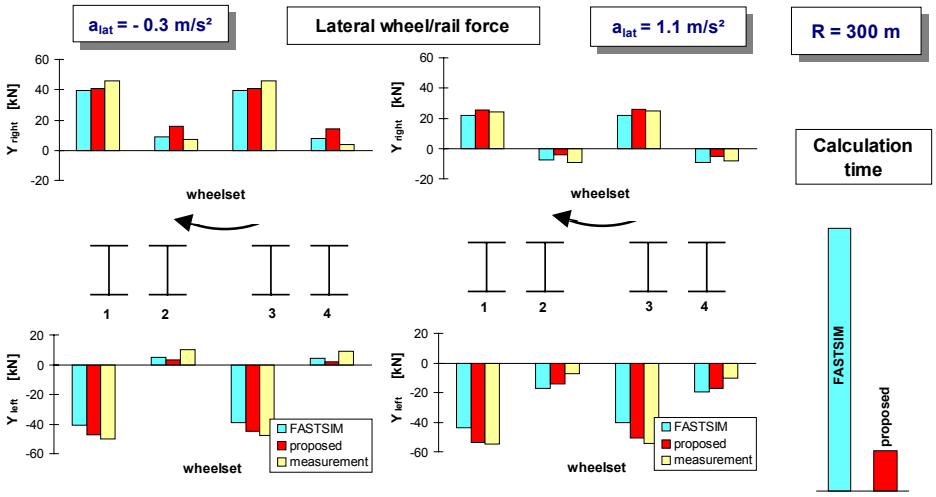

Fig. 1. Measured lateral wheel-rail forces in a curve with 300 m radius compared with the simulations using the method developed by the author [8] and using FASTSIM.

The results using both calculation methods mentioned are similar, see Fig. 1. However, there is a significant difference in the calculation time. The results computed using the proposed method show good agreement with the measurements. Especially in the case of the leading wheelsets, they are nearer to the actually measured values than the results obtained in the simulations using FASTSIM.

3. DIFFERENCES BETWEEN THE VEHICLE DYNAMICS AND AXLE DRIVE DYNAMICS

Depending on the aim of the tests, different measured creep-force functions can be found in the literature [6]. Because of the variety of measurements different models are used for the same physical phenomenon - forces between wheel and rail - in the vehicle dynamics and axle drive dynamics (Fig. 2). How is this possible? The reason for this are different fields of parameters and different areas of investigations.

In the vehicle dynamics small creep values are of main importance. Tangential forces in longitudinal as well as in lateral directions influence the vehicle behaviour, therefore longitudinal and lateral creep as well as spin should be taken into account. Based on the theory of rolling contact, the creep forces depend on the creep as non-dimensional value. The friction coefficient is assumed to be constant. The difference

between dry and wet conditions is usually expressed only with the value of friction coefficient and not with a change of the creep-force function gradient.

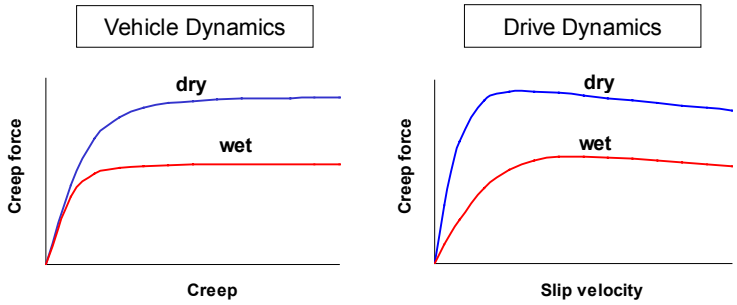

Fig. 2. Differences between the typical creep-force functions used in the vehicle dynamics and in axle drive dynamics.

In the drive dynamics large values of longitudinal creep influence its behaviour. In the simulated systems usually only the longitudinal direction is taken into account. Based on the experiments, the creep forces are usually assumed as dependent on the slip velocity between wheel and rail. There is a maximum of creep-force function, so called adhesion optimum, and a decreasing section behind this maximum. The gradient and the form of creep-force functions for wet, dry or other conditions are different.

4. MODEL OF WHEEL-RAIL FORCES USEFUL FOR SIMULATION OF VEHICLE DYNAMICS AND AXLE DRIVE DYNAMICS INTERACTION

For the complex simulation of dynamic behaviour of locomotive or traction vehicle in connection with drive dynamics and traction control, high longitudinal creep and decreasing section of creep-force function behind the adhesion limit has to be taken into account. The different wheel-rail models described above have to be made into one model, which is suitable for both vehicle dynamics and drive dynamics simulations.

A creep-force law with a marked adhesion optimum can be modelled using the friction coefficient decreasing with increasing slip (creep) velocity between wheel and rail. The dependence of friction on the slip velocity was observed by various authors and is described e. g. in [6], [9]. The variable friction coefficient can be expressed by the following equation

$$f = f_0 \cdot \left[(1 - A) \cdot e^{-B \cdot w} + A \right] \qquad (6)$$

where f_0 - maximum friction coefficient
w - magnitude of the slip (creep) velocity vector [m/s]

B - coefficient of exponential friction decrease [s/m]

A - ratio of limit friction coefficient f_∞ at infinity slip velocity to maximum friction coefficient f_0

$A = f_\infty / f_0$.

From the point of view of tractive effort and traction dynamics the creep law for bad adhesion conditions is of main importance: wet rail and surface pollution e. g. oil, dirt, moisture. Even for dry conditions the gradient of creep-force functions is usually lower than the theoretical value. The reason of this is the layer of moisture, which can be taken into consideration in the "stiffness coefficient" of surface soil [4]. In the vehicle dynamics, this real conditions are taken into account simply with a reduction of Kalker's creep coefficients [2]. This method is used for the linear creep force law but can be used generally as well.

The combination of

- the friction coefficient as a function of slip velocity between wheel and rail and
- the reduction of Kalker's creep coefficients

allows

- on the one hand to achieve the form of creep-force function with an adhesion optimum as known from measurements and as necessary for traction investigations
- and on the other hand to keep the principles of creep forces computation in dependence on longitudinal and lateral creep and spin.

In this manner, the creep-force functions can be adapted for various conditions of wheel-rail contact, see Fig. 3. The diagrams show the adhesion coefficient $\mu_x = F_x/Q$ in function of longitudinal creep s_x.

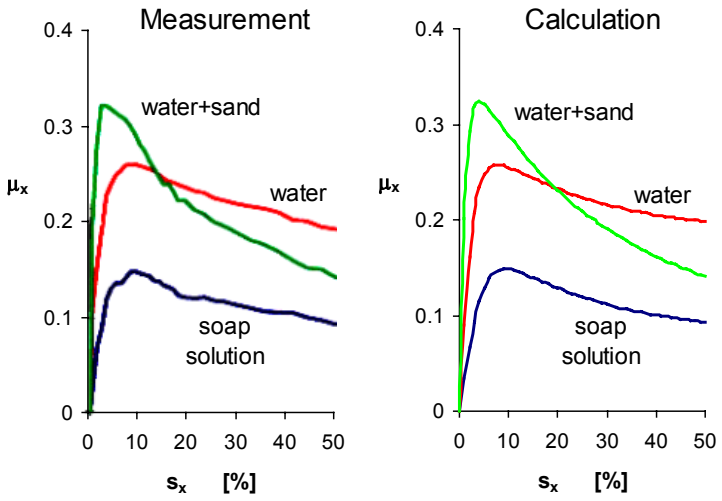

Fig. 3. Modelling of various adhesion conditions using the friction coefficient as function of slip velocity between wheel and rail (measurement: adhesion tests with the SBB 460 locomotive, V = 20 km/h).

At the same time, using this principle, the adhesion maximum decreases and parallel to this the creep value at this maximum decreases with increasing of vehicle speed V, which is a phenomenon well known from measurements. It can be observed on Fig. 4, which shows example of creep-force functions modelled using the method according to Polach [8] with the extension described above. The same principles can

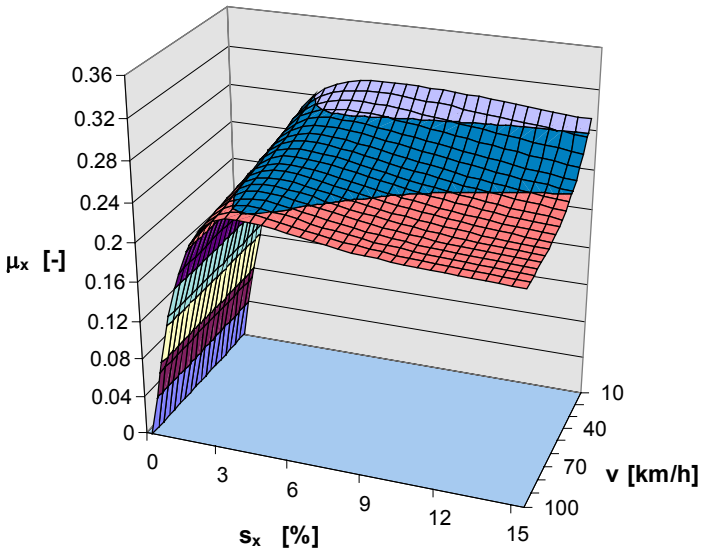

Fig. 4. Influence of vehicle speed on the form of creep-force functions using the friction coefficient as function of slip velocity between wheel and rail.

be used to extend the model of wheel-rail forces based on FASTSIM or any other method of creep force computation.

Although the method described above allows to reproduce the basic tendencies of measured creep-force functions at large creep values, there are some limitations. To achieve the adhesion optimum at large creep values, a significant reduction of Kalker's coefficients would be necessary (less than 0.1). But the measurements of the creep-force function gradient do not usually show so low values.

The explanation may lie in the combination of dry and wet friction. For small creep values, the area of adhesion extends to the greater part of the contact area. The conditions are similar to dry friction. For large creep values, there is slip in the main part of the contact area. The layer of water or pollution influences the resultant force. The "stiffness coefficient" of surface soil decreases and, as a result of this, the creep-force function changes its gradient significantly.

In spite of the complexity of this phenomenon, a good possibility was found to model the wheel-rail contact forces in good agreement with the measured functions using a simple extension of the method developed by the author [8]. In this method

the tangential forces (equation (2)) are expressed as a function of the gradient ε of the tangential stress (equation (5)). Using a reduction of Kalker's coefficient with a factor k, the equation (5) has the form

$$\varepsilon_R = \frac{1}{4}\,\frac{G\cdot\pi\cdot a\cdot b\cdot k\cdot c_{11}}{Q\cdot f}\,s_x = k\cdot\varepsilon \qquad (7)$$

In (2) there are two terms: one of them connected to the area of adhesion, another one to the area of slip. Using different reduction factors k_A in the area of adhesion and k_S in the area of slip, the equation (2) has the form

$$F = -\frac{2\cdot Q\cdot f}{\pi}\left(\frac{k_A\cdot\varepsilon}{1+(k_A\cdot\varepsilon)^2} + \arctan(k_S\cdot\varepsilon)\right) \qquad (8)$$

Using $k_A > k_S$, there is nearby no reduction of the creep-function gradient at small creepages but a significant reduction of the gradient near saturation. The gradient of the creep-force function at the co-ordinate origin corresponds to the reduction of Kalker's coefficient

$$k = \frac{k_A + k_S}{2} \qquad (9)$$

The creep-force functions are shown in Fig. 5 for a constant coefficient of friction. Using the proposed method with two reduction factors, the form of the creep-force functions is more similar to the form of measured functions than using one reduction factor k, see Fig. 5. The diagrams show creep-force functions for longitudinal direction in non-dimensional co-ordinates

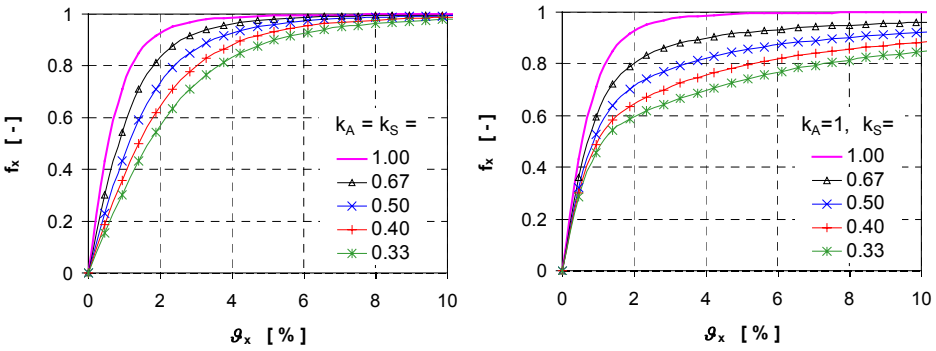

Fig. 5. Reduction of Kalker's coefficients: the standard method (left) and the proposed method with two different reduction factors (right).

- non-dimensional wheel-rail force

$$f_x = \frac{F_x}{Q \cdot f} \tag{10}$$

- non-dimensional longitudinal creep

$$\vartheta_x = \frac{G.a.b.c_{11} \cdot s_x}{Q \cdot f} \tag{11}$$

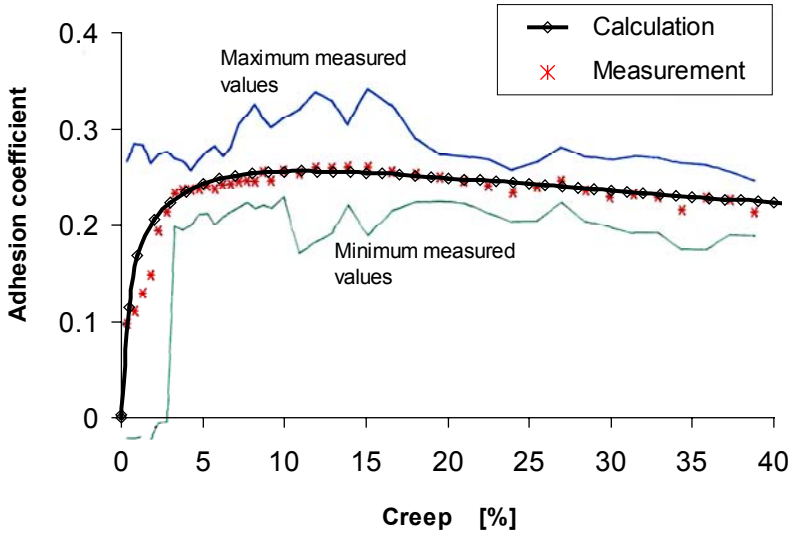

Fig. 6. Model of wheel-rail contact forces based on the measurements with the Adtranz SBB 460 locomotive (7 measurements on wet rails; V = 40 km/h; model parameters: k_A = 0.16, k_S = 0.07, f_0 = 0.305, A = 0.50, B = 0.16 s/m).

Using the proposed method various measured creep-force functions were modelled. Fig. 6 shows measurements with the Adtranz SBB 460 locomotive. There are results of 7 measurements with speed of 40 km/h on wet rail. The measured points were classified and average values, maximal and minimal values were calculated. Using the model described, parameters were found which provide a creep-force model with a very good agreement with the measurements.

Another example in Fig. 7 shows measurements with the Siemens Eurosprinter locomotive No. 127 001 (according to [1]). Changing the parameters a very good agreement of the measured and modelled dependence can be achieved again.

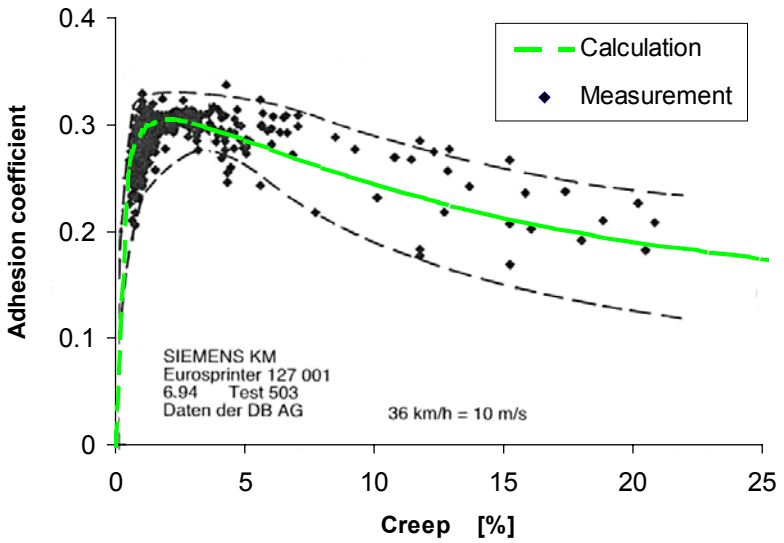

Fig. 7. Model of wheel-rail contact forces based on the measurements with the Siemens locomotive Eurosprinter 127 001 [1] (rail conditions not mentioned; V = 36 km/h; model parameters: $k_A = 0.72$, $k_S = 0.36$, $f_0 = 0.36$, $A = 0.38$, $B = 0.70$ s/m).

The wheel-rail models with parameters presented above were tested for various speeds and for range of longitudinal creep from very small to high creep values. Even in this large range the results are plausible and the model is not limited to one speed or to a small creep range. Of course, change of conditions in contact of wheel and rail as well as other effects, e. g. the cleaning effect due to large creep (so called rail conditioning) will cause change of wheel-rail model parameters.

The examples confirm that the method gives a very good possibility to model the functionality of wheel-rail contact necessary for the investigation of axle drive systems. Parallel to this the method allows to keep the principles of creep forces computation in dependence on longitudinal and lateral creep and spin, which is necessary for vehicle dynamics investigations.

5. APPLICATION EXAMPLES WITH THE PROPOSED WHEEL-RAIL MODEL

As an application example of the proposed wheel-rail model, two cases will be presented

- Quasi-static and dynamic investigations of the influence of locomotive traction effort on the wheel-rail forces and curving behaviour
- Influence of traction control on locomotive dynamic behaviour using co-simulation of ADAMS/Rail and MATLAB/SIMULINK.

5.1. Influence of Locomotive Tractive Effort on the Curving Behaviour

In order to verify the method of wheel-rail forces computation, the ADAMS/Rail model of the SBB 460 locomotive was extended by a full model of the driving system and runs through a curve on wet rails were simulated.

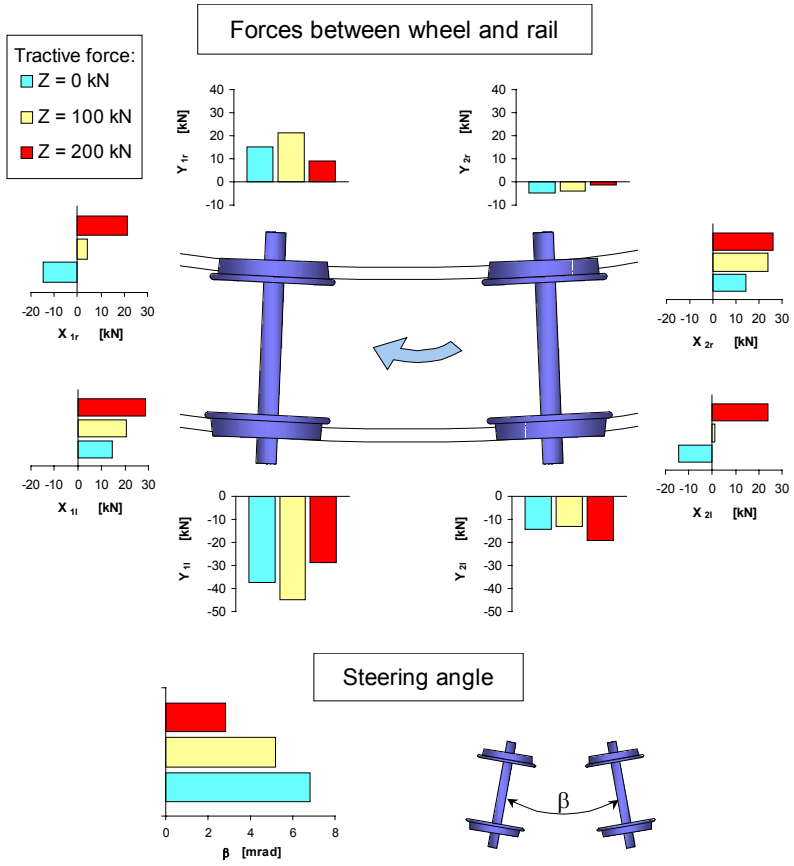

Fig. 8. Longitudinal and lateral wheel-rail forces and steering angle between wheelsets for different tractive effort.

Fig. 8 shows the distribution of longitudinal and lateral quasi-static wheel-rail forces in a curve of 300 m radius, running at a speed of 87.7 km/h (lateral acceleration a_{lat} = 1.0 m/s²). The wheel-rail forces change with increasing tractive effort. Without tractive effort, there are opposite longitudinal forces on the left and right wheel. With increasing tractive effort the longitudinal forces on the outer wheel of the first wheelset and on the inner wheel of the second wheelset increase. An even distribution of the longitudinal forces will be achieved first on the adhesion limit. The angle between the wheelsets in the horizontal plane (so called steering angle) depends on the tractive effort as well.

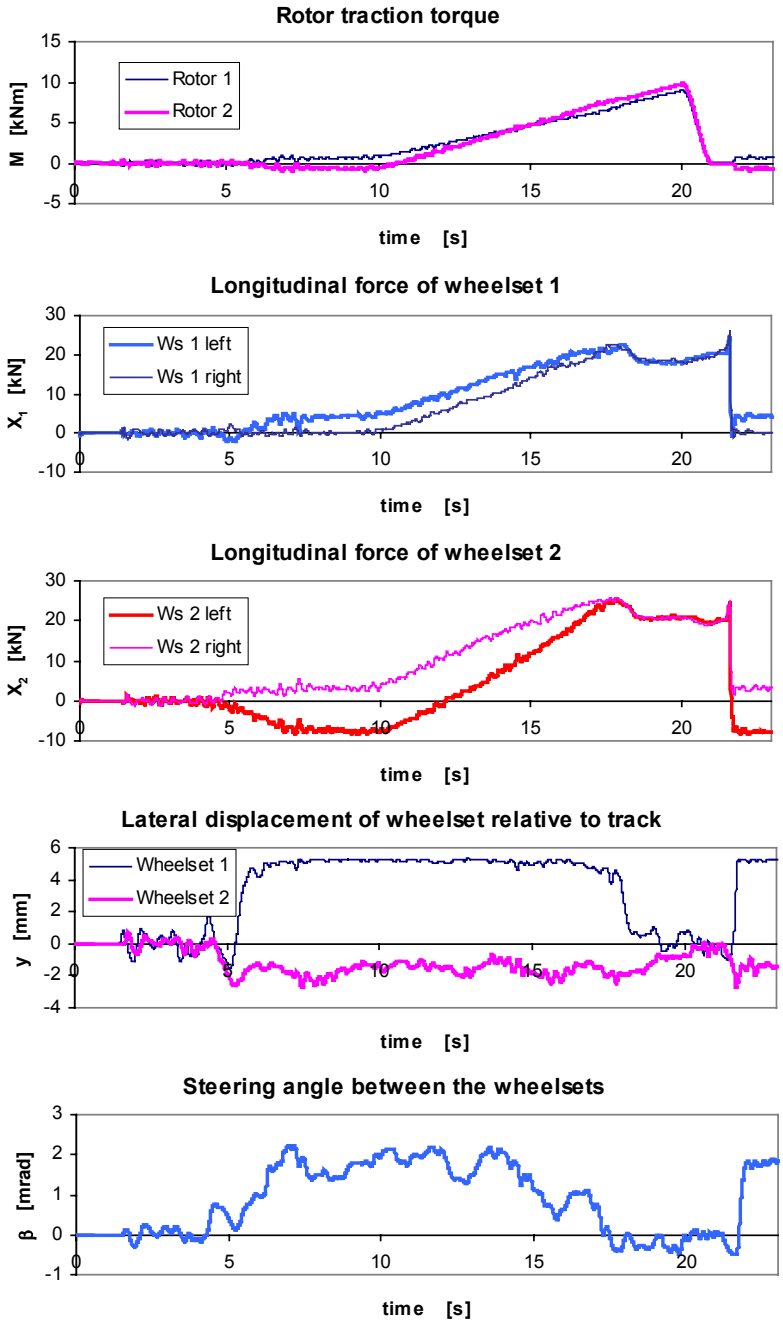

Fig. 9. Time plots of adhesion test simulation (curve radius R = 400 m, speed V = 70 km/h).

Without tractive effort, the angle between the wheelsets achieves the maximal value due to the steering moment of longitudinal forces. With increasing tractive effort the distribution of longitudinal forces changes as explained before, the steering moment acting on the wheelsets decreases and the steering angle between the wheelsets decreases as well. In spite of this the experience with these locomotives confirms that there is no negative influence on the wear of wheels and rails because of the statistically rare occurrence of maximal tractive effort. On the Gotthard-route the locomotives achieve 3 to 4 times longer intervals between the renewals of wheel profiles than the previous ones [13].

In order to test the possibility of simulating the dynamic change of traction torque, a test case used during the adhesion test was simulated. In the course of curving simulation, the traction torque was increased from zero to the adhesion limit, in a similar way as during the adhesion test measurements. In this manner, a run on the unstable (decreasing) section of creep-force function was simulated. The influence of increased tractive effort on longitudinal and lateral wheel-rail forces and the steering angle between the wheelsets of a single bogie were investigated. The simulation results show the same behaviour as observed during the tests. The time plots of traction torque, longitudinal wheel-rail forces, lateral displacements of the wheelsets relative to track and steering angle between wheelsets for the speed of 70 km/h are shown in Fig. 9. With increasing tractive effort, the wheelset steering ability

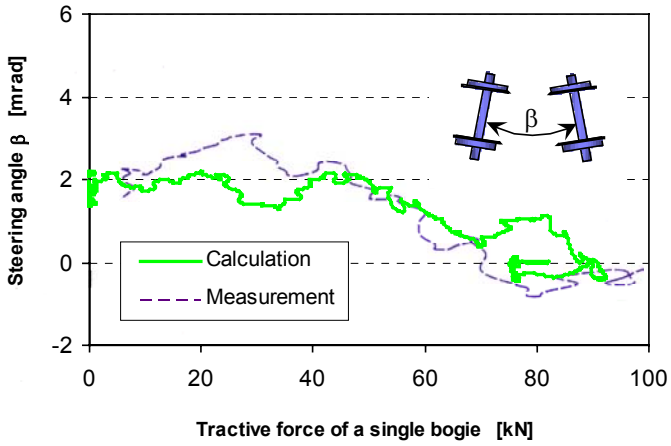

Fig. 10. Comparison of the measured and calculated steering angle between wheelsets as function of tractive effort of a single bogie.

decreases. Simultaneously, the first wheelset of the bogie moves to the inner rail. The calculation shows the same dynamic behaviour tendency due to the change of the tractive effort as observed during the tests. The calculated steering angle as a function of tractive force in the steering linkages is compared with the measurement in Fig. 10. The comparison confirms a good agreement in the tendency although the simulated track irregularity does not correspond to the reality.

5.2. Influence of Traction Control on Locomotive Dynamic Behaviour

The traction control influences possible tractive effort as well as the dynamic behaviour of the locomotive. Because of different simulation tools used in traction control and in vehicle dynamics, a co-simulation was chosen as a way to investigate this mechatronic system. The control part of the locomotive modelled in MATLAB/SIMULINK comprises the motor control and the adhesion control. The motor control is represented by measured transfer functions and the adhesion control is represented by SIMULINK blocks.

The adhesion controller uses an adaptive control system [10] which determines the optimal longitudinal slip. The control is based on the rotor velocity response to the torsion oscillations, excited by a test signal superimposed to the motor torque. Based on the filtered sinusoidal rotor velocity, the gradient of the creep-force function is computed. The adhesion optimum is achieved when the gradient of creep-force function is zero.

The ADAMS/Rail model of the SBB 460 locomotive described above was connected with the control unit in MATLAB/SIMULINK and the system was investigated using co-simulation. The input values of the ADAMS/Rail model consisted of the torque of the motors, and the input values of the control unit in MATLAB/SIMULINK were the angular velocities of the rotors and the desired motor torque value.

As an example of computed results a simulation of locomotive starting and acceleration is presented. The track consists of a short straight, a right curve with $R = 300$ m, another short straight and another right curve with $R = 385$ m. Fig. 11 shows the following computed values in function of the distance along the track

- Locomotive speed
- Torque of rotor 1 and 2
- Longitudinal forces of the first wheelset
- Lateral forces of the first wheelset
- Steering angles between the wheelsets of the first and second bogie.

The rotor torque oscillations due to the test signal can be seen in the results. Because only the first bogie provided the tractive effort, a difference in the steering angle of the first and second bogie due to traction can be observed. At the same time there are changes in the longitudinal and lateral wheel-rail forces due to track curvature and due to increasing vehicle speed.

The results of presented application examples confirm this as a possible way for the simulation of complex problems of vehicle dynamics, axle drive dynamics and traction control. The next step will be an optimisation of locomotive behaviour using a model, which contains mechanics, electrics and controls.

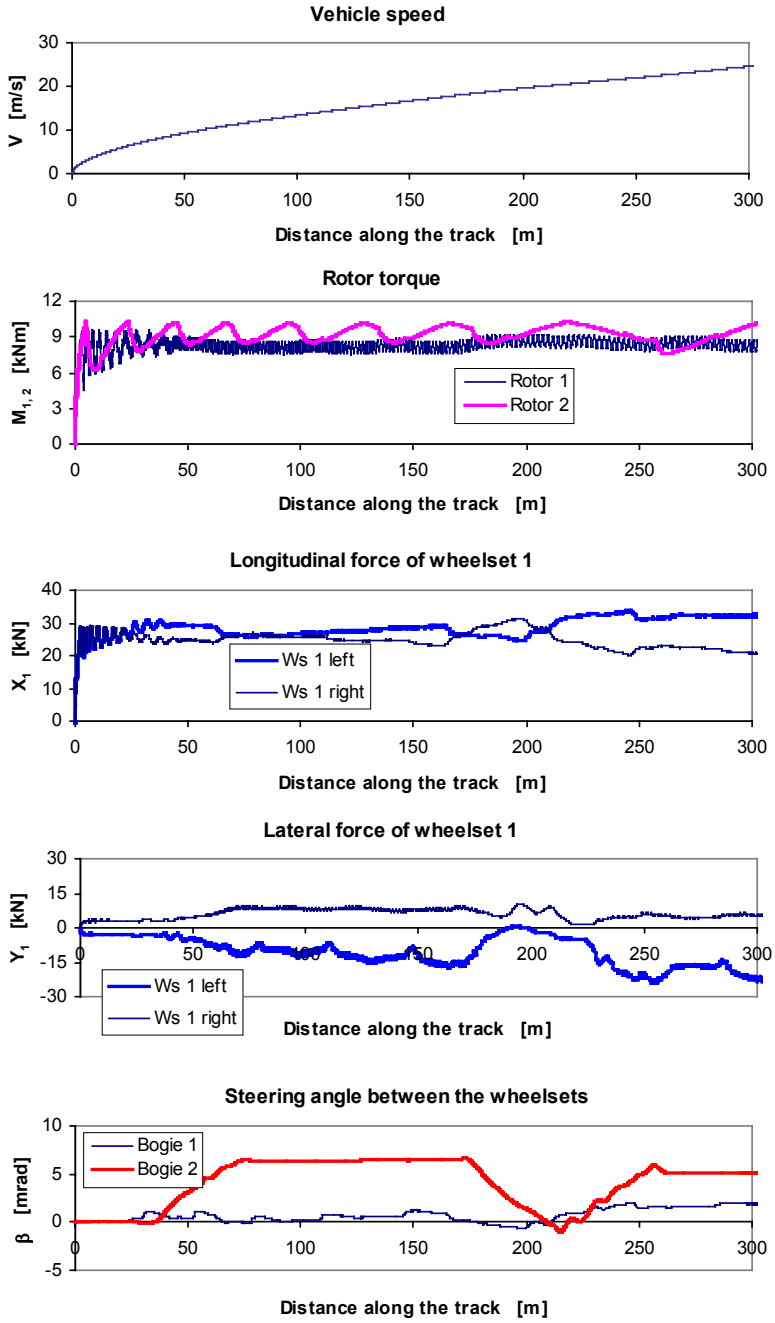

Fig. 11. Starting and acceleration of a locomotive under difficult adhesion conditions on curved track resultant from ADAMS/Rail and MATLAB co-simulation.

5. CONCLUSION

To investigate a mechatronic system of railway traction vehicles, e. g. influence of traction control and vehicle dynamics on the forces between wheel and rail, an adaptation of wheel-rail forces model is necessary. A fast method for the computation of wheel-rail forces developed by the author was extended to simulate various wheel-rail adhesion conditions. The proposed method is suitable for the investigations of problems regarding the traction control and axle drive dynamics and their interaction with vehicle dynamic behaviour. The results calculated using the proposed method show good agreement with measurements and confirm this as a possible way for the simulation of complex mechatronic systems of railway vehicles.

REFERENCES

1. Engel, B., Beck, H. P., Alders, J.: Verschleißreduzierende Radschlupfregelung mit hoher Kraftschlussausnutzung. Elektrische Bahnen, Vol. 96 (1998), No. 6, pp.201-209
2. Kalker, J. J.: On the rolling contact of two elastic bodies in the presence of dry friction. Thesis, Delft 1967
3. Kalker, J. J.: A fast algorithm for the simplified theory of rolling contact. Vehicle System Dynamics 11(1982), pp. 1-13
4. Kalker, J. J.: Über die Mechanik des Kontaktes zwischen Rad und Schiene. ZEV-Glasers Annalen 102 (1978), pp. 214-218
5. Kalker, J. J.: Three-dimensional elastic bodies in rolling contact. Kluwer Academic Publishers, Dordrecht, Netherlands 1990
6. Polach, O.: On problems of rolling contact between wheel and rail. Archives of Transport. Polish Academy of Sciences, Vol. 2 (1990), No. 4, pp. 311-330
7. Polach, O.: Solution of wheel-rail contact forces suitable for calculation of rail vehicle dynamics. Proc. of the 2nd Int. Conference on Railway Bogies, Budapest, Sept. 14-16, 1992, pp. 10-17
8. Polach, O.: A Fast Wheel-Rail Forces Calculation Computer Code. Proc. of the 16th IAVSD Symposium, Pretoria, August 1999, Vehicle System Dynamics Supplement 33 (1999), pp. 728-739
9. Rabinowicz, E.: Friction and wear of materials. John Wiley and Sons, New York, 1965
10. Schreiber, R., Kögel, R.: Identifikationsmethode zur Bestimmung der Adhäsion zwischen Rad und Schiene. ZEV+DET Glasers Annalen, Vol. 120 (1996), No. 2, pp. 48-54
11. Shen, Z. Y., Hedrick, J. K. and Elkins, J. A.: A comparison of alternative creep force models for rail vehicle dynamic analysis. Proc. of the 8th IAVSD-Symposium, Cambridge, MA, August 15-19, 1983, pp. 591-605
12. Vermeulen, P. J., Johnson, K. L.: Contact of non spherical bodies transmitting tangential forces. Journal of Applied Mechanics, Vol. 31 (1964), pp. 338-340
13. Müller, R.: Veränderungen von Radlaufflächen im Betriebseinsatz und deren Auswirkungen auf das Fahrzeugverhalten (Teil 1). ZEV+DET Glasers Annalen, Vol. 122 (1998), No. 11, pp. 675-688